Clays and Clay Minerals, Vol. 39, No. 1, 14–21, 1991.

MERCURY ADSORPTION BY SULFURIZED FIBROUS SILICATES

L. DAZA,[1] S. MENDIOROZ,[1] AND J. A. PAJARES[2]

[1] Instituto de Catálisis y Petroleoquímica
C.S.I.C. Serrano 119, 28006 Madrid, Spain

[2] Instituto del Carbón, C.S.I.C.
La Corredoria, s/n. Oviedo, Spain

Abstract—To eliminate mercury vapor from gas streams, three major methods are used: condensation, absorption, and adsorption. This work deals with adsorption, using elemental sulfur as an active phase supported on sepiolite and palygorskite fibrous clays. Sulfur loads of 5–30% were deposited by catalytic oxidation of hydrogen sulfide at temperatures of <200°C, the clays acting first as a catalyst of the reaction and then as a carrier of the obtained sulfur. The ability of the sulfurized clay adsorbents to retain mercury was studied at 45°C and 1 mm Hg pressure. The high values found, about 4 g Hg/g S supported on clays, compared with 1.69 g Hg/g S on activated carbon under the same conditions are related to a more appropriate pore size distribution, with more of the pore widths >6 nm for the sulfurized silicates. Also, the allotropic state of the deposited sulfur, where Sπ (octo-catena) is better than Sλ (octo-cycle), may also be a contributing factor.

Key Words—Activated carbon, Adsorption, Mercury, Palygorskite, Pore size distribution, Sepiolite, Sulfurized silicates.

INTRODUCTION

Mercury is a powerful poison, not only for human beings but also for industrial gas streams. In the former, mercury reacts with thiol-containing enzymes, thereby blocking their activity; in the latter, the presence of mercury shortens, by amalgamation, the life of the mechanical parts of equipment and degrades the metallic catalysts involved in the chemical processes. Significant amounts of mercury can be found in hydrogen streams emanating from chloro-alkali manufacturing plants; the quantities depend on the temperature of the gases. Mercury is also present in effluents from roasting sulfide ores in amounts ranging from 40 to 200 ppm, depending on the origin and purity of the feed involved. Fossil fuels such as petroleum, natural gas, or coal, contain some mercury (~0.2 ppm), which can be inhaled by human beings or transformed via a complicated biological cycle into alkyl-mercury derivatives, much more dangerous than the original mercury itself.

Mercury must therefore be removed or, at least, its concentration must be decreased to the levels below those stipulated by regulatory agencies (threshold limit value (TLV) set up by the American Conference of Governmental Industrial Hygienist in 1987–1988 (ACGIH, 1987–1988) 0.1 mg/m^3) before such industrial streams can be safely used.

The various methods that have been developed to reduce the level of Hg in industrial streams can be grouped in physical (condensation), chemical (absorption), and physiochemical (adsorption) processes. The actual method adopted depends on the available facilities, the initial mercury content in the gaseous streams, and the final level to be reached; its cost will be inversely related to the desired final level. In general, adsorption is the most suitable method if small concentrations (<500 ppm) and final levels of <0.001 ppm are the challenge.

Sulfurized active carbon has been extensively studied as an adsorbent (Sinha and Walker, 1972; Lovett and Cunniff, 1974; Steijns and Mars, 1974) and developed by companies, such as Norit and Montedison, but drawbacks are its high cost and low possibilities of mercury recovery once the adsorbent is saturated. In the development of a less expensive and more recoverable adsorbent, some natural or slightly treated silicates appear to be promising materials, because they possess a developed network of pores and a large surface area. Moreover, the clays have the advantage of a much lower cost and higher thermal stability than activated carbon, which enables mercury recovery by dry distillation (~560°C) or roasting.

Daza *et al.* (1987) described a general mechanism of sulfurization and demercurization using granular diatomite, a texturally and structurally uncomplicated noncrystalline silica having a significant macropore content and low surface reactivity. In the present work, the study has been extended to the fibrous silicates sepiolite and palygorskite, which possess inter- and intra-particle porosity and high surface reactivity. The work deals first with the preparation of sulfurized adsorbents and second with the influence of textural and structural parameters of the sulfurized samples in their mercury-scavenging capacity.

EXPERIMENTAL

Equipment and methods

Elemental analyses were made in a Perkin Elmer 3030 AA spectrophotometer, working in the emission

Copyright © 1991, The Clay Minerals Society

https://doi.org/10.1346/CCMN.1991.0390102 Published online by Cambridge University Press

Table 1. Chemical analysis of raw materials (wt. %).[1]

	SB	SPG	SPS	PN	PT
SiO_2	59.39	60.35	60.31	60.36	63.70
Al_2O_3	3.74	3.44	5.16	13.44	12.42
Fe_2O_3	0.69	0.81	1.05	4.72	3.16
MgO	18.06	18.42	16.64	4.74	3.56
CaO	1.46	1.05	0.49	1.48	0.07
Na_2O	4.72	4.05	4.92	1.19	2.05
K_2O	1.08	0.91	1.60	1.40	1.75
L.O.I.	10.85	10.98	9.83	12.68	13.28

[1] For sample description, see text.

mode, for Na, K, and Ca and in the absorption mode for the rest of the cations. Flame, lamps, and slit width were those recommended by the manufacturer for routine work. Analyses were performed after acid digestion of the samples with HF (38%) in a PTFR autoclave following Langmhyr and Paus (1968). The total sulfur content was determined in a conventional LECO SC-32 No. 780-600 apparatus.

All starting materials and products were identified by X-ray powder diffraction (XRD) using a Philips PW 1710 powder diffractometer and CuKα radiation.

Surface area and porosity of the samples were calculated from N_2 adsorption-desorption isotherms, the data acquired in a Digisorb 2600 equipment at 77 K, and mercury penetration porosimetry effected in a PoreSizer 9310 equipment, both from Micromeritics. Surface areas were calculated from the first part of the isotherms ($p/p_0 < 0.3$) using 0.162 nm^2 as cross-sectional area of the adsorbed nitrogen molecule. Mesopore distribution was calculated from the adsorption branch of the isotherm by the Pierce method (1953). Micropore analysis was made by the MP method from Brunauer *et al.* (1973).

The morphology of the samples was studied in a ISI DS-130 scanning electron microscope coupled to a Si/Li detector equipped with a Be window. A small amount of powder was glued to a graphite stub and coated with a thin Au/Pd film. Eventually, semiquantitative energy-dispersive X-ray (EDX) analyses were made on the samples from spots about 1 μm in diameter. Because of the apparent overlapping of the S Kα and Hg Lα lines, a gaussian deconvolution method for quantification was used.

The capacity for adsorbing mercury was studied in the static system described by Steijns *et al.* (1976), as modified by Daza (1986). The system consisted of a mercury-containing device mounted on top of an ordinary dessicator attached to a vacuum pump, which ensured a total mercury pressure inside the dessicator of <1 mm Hg. The equipment was placed in a furnace and kept at a constant temperature of 45°C. The samples were deposited inside the desiccator and weighed every 3–4 days until mercury uptakes of <1% were observed (~20 days).

Raw materials

Three sepiolite and two palygorskite samples supplied by Tolsa, S.A. were used in the work. The sepiolite samples included a natural, untreated sample containing >95% pure mineral, 0.2–0.4 mm aggregate size, designated here as SB and two products from this sample resulting from wet (SPG) and dry (SPS), respectively, micronization treatments. The palygorskite samples were, a natural 0.2-μm particle size sample (PN) and its acid-treated (at reflux) product, PT. All samples were characterized by the methods mentioned above; their chemical composition and textural parameters are shown in Tables 1 and 2, respectively.

Adsorbents

Five series of 4–5 samples each having sulfur loads of 5–30% were prepared by catalytic oxidation of hydrogen sulfide at low temperature (<200°C) in a fixed-bed reactor (Mendioroz *et al.* 1986). The clays acted as a catalyst for the reaction $n(H_2S) + n/2\ O_2 \rightarrow S_n + nH_2O$ and were coated with the resulting sulfur as the reaction progressed. The process was continued until the desired sulfur charge was loaded on the samples. The sulfurization time depended on the solid surface reactivity, 1–9 hr for palygorskite, 1–18 hr for sepiolite. All five sample series are herein designated by the cap-

Table 2. Textural parameters of raw materials.[1]

	SB	SPG	SPS	PN	PT
S_{BET} (m^2/g)	337	364	298	117	137
C_{BET}	233	151	180	115	219
V_p (cm^3/g)	0, 546	0, 640	0, 602	0, 268	0, 322
r (Å)	33	35	40	46	47
$V_{\mu p}$ (mm^3/g)	70	60	61	11	6
$r_{\mu p}$ (Å)	5	5	5	6	5
V_M (cm^3/g)	0, 138	1, 240	1, 796	1, 406	1, 351
R_M (Å)	719	1727	1574	1666	862

[1] For sample identification, see text. S_{BET} = Surface area from N_2 adsorption (BET eq.); C_{BET} = BET constant; V_p = Meso- and micropore volume (d < 500 Å) calculated from total N_2 uptake at $p/p_0 = 0.98$; r = Average radius for meso and micropores = 20,000 V_p/S_{BET}; $V_{\mu p}$ = Micropore volume (d < 20 Å) from application of MP method (see text); $r_{\mu p}$ = Average micropore radius; V_{MP} = Macropore volume (d > 500 Å) from mercury intrusion porosimetry; R_{MP} = Average macropore radius.

https://doi.org/10.1346/CCMN.1991.0390102 Published online by Cambridge University Press

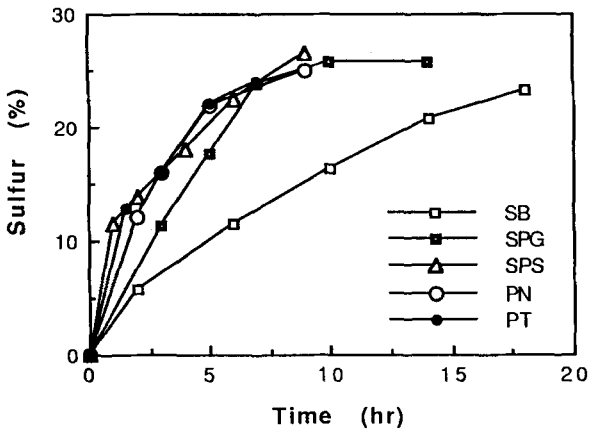


Figure 1. Sulfur uptake vs. time: □ SB; ■ SPG; △ SPS; ○ PN; ● PT.

ital letters corresponding to each material followed by a digit (1, 2, 3, 4, 5) related with their sulfur content (%).

RESULTS

The progress of sulfur uptake vs. time can be seen in Figure 1. The sulfur content and the variation in the textural parameters produced by the deposited sulfur are listed in Tables 3 and 4.

The following can be inferred from the data regarding the effect on samples of increasing sulfur loads:

1. A dramatic loss in surface area was noted for all samples with the first deposition of sulfur; afterwards a steady decrease in surface area was apparent. The effect was less significant in palygorskite samples.
2. The BET constant, an important parameter in understanding the reactivity of the solid for nitrogen adsorption, abruptly decreased with the first sulfur deposition, reaching an almost constant value for all samples as sulfur load increased, in spite of the different raw materials used. This means that N_2 was adsorbed on increasingly similar surfaces (S covered) and, hence, that a coating of sulfur spread on the solid until it was totally covered. The differences in reactivity and structure shown among the original materials were not preserved; only a sulfur surface was later exposed to the incoming gases.
3. Microporosity, at least that accessible to N_2 and S, was not significant for these samples, but the initial deposition of sulfur on top of the bundles of fibers and therefore on the micropore mouths blocked the entrance to new sulfur loads, resulting in important changes in surface area.
4. The mesoporosity decreased progressively; sulfur was first deposited on active centers of the pore walls through a surface reaction (Daza *et al.*, 1989) spreading over the walls and finally covering the entire surface. After the first monolayer, subsequent layers were accumulated until the pores were completely filled.
5. Macroporosity was very significant in the raw materials especially in the micronized samples (see Table 2). Two different patterns were noted with respect to the effect of sulfur deposition: (1) for untreated sepiolite and palygorskites, sulfur deposition caused a gradual decrease in macroporosity similar to that found in mesoporosity, due most probably to the same monomultilayer mechanism; (2) for the SPG and SPS series, massive deposition of sulfur on the network of criss-crossing fibers resulted in the formation of a sulfur "shell" and, as

Table 3. Sulfur content and textural parameters[1] of sepiolite adsorbents.[2]

Sample	S (%)	S_{BET} (m^2/g)	C_{BET}	V_p (cm^3/g)	r (Å)	$V_{\mu p}$ (mm^3/g)	$r_{\mu p}$ (Å)	V_M (cm^3/g)	R_M (Å)
SB1	5.72	127	65	0.449	71	18	5	0.106	644
SB2	11.45	81	79	0.380	94	18	5	0.094	608
SB3	16.42	73	90	0.357	98	9	5	0.080	649
SB4	20.68	60	96	0.299	99	5	7	0.076	583
SB5	23.28	53	92	0.277	105	14	5	0.014	555
SPG1	11.43	78	112	0.305	79	2	5	0.101	776
SPG2	17.64	59	121	0.254	86	1	5	0.093	762
SPG3	23.88	51	106	0.222	87	6	5	0.047	863
SPG4	25.77	55	85	0.230	84	2	5	0.061	709
SPG5	25.86	40	90	0.176	88	7	5	0.060	707
SPS1	11.63	80	81	0.314	78	14	5	0.043	603
SPS2	13.76	75	89	0.290	77	8	5	0.049	622
SPS3	18.10	68	99	0.273	80	3	5	0.024	531
SPS4	22.41	49	97	0.197	80	3	5	0.030	557
SPS5	26.60	37	96	0.165	89	3	5	0.025	538

[1] Abbreviations as in Table 2.
[2] For sample identification, see text.

https://doi.org/10.1346/CCMN.1991.0390102 Published online by Cambridge University Press

Table 4. Sulfur content and textural parameters[1] of palygorskite adsorbents.[2]

Sample	S (%)	S_{BET} (m^2/g)	C_{BET}	V_p (cm^3/g)	r (Å)	V_{ap} (mm^3/g)	r_{ap} (Å)	V_M (cm^3/g)	R_M (Å)
PN1	12.11	54	96	0.204	76	3	5	0.928	1370
PN2	15.92	49	86	0.200	82	2	6	0.824	1333
PN3	21.89	45	73	0.191	85	0.8	5	0.680	1175
PN4	25.02	42	68	0.161	77	0.3	5	0.692	1341
PT1	12.88	75	89	0.242	64	2	6	1.067	864
PT2	16.04	70	87	0.231	66	2	6	1.024	869
PT3	22.14	64	81	0.194	61	1	6	0.992	874
PT4	23.99	50	79	0.183	73	0.03	6	0.883	821

[1] Abbreviations as in Table 2.
[2] For sample identification, see text.

a consequence, in the almost total disappearance of macroporosity. This shell hindered further gas diffusion inside the solid.

Mercury adsorption

Figures 2 and 3 show the mercury adsorption curves for all five series. Black metacinnabar (HgS) was the only species formed after mercury chemisorption, as was verified by XRD. No mercury was retained in the raw materials used as a blank. Equilibrium data after 20 days exposure are listed in Tables 5 and 6; the mercury retained by sulfurized activated carbon from NORIT sample RBS1 is also included as a reference.

Specific activity (Ac), calculated as grams of mercury retained per gram of sulfur, the maximum value attainable being 6.25, is shown in column 6. The values show that most of the samples gave yields as high as 50%, much greater than sample RBS1 (Ac = 1.69). In general, mercury retention, as well as the unreactive fraction of sulfur of the adsorbents, increased, whereas the specific activity decreased with the sulfur load.

DISCUSSION

Influence of texture

Sepiolite is composed of bundles of fibers 1–2 μm long which possess significant interparticular mesoporosity. The micronization treatment disaggregated the particles and produced elongated, isolated fibers criss-crossing to form a thick meshwork on which sulfur was easily deposited. The deposition of sulfur lowered the macroporosity of the samples drastically (see also, Daza *et al.*, 1989). The original particles of palygoskite were about 0.2 μm in size and aggregated to form secondary particles having a significant macroporosity. Treatment with acid resulted in the rupture of the fibers, as well as in the removal of impurities and exchangeable cations, slightly enhancing the po-

Table 5. Mercury adsorption of sepiolite-based adsorbents.[1]

Sample[2]	S (%)	S_{cal} (m^2/g)[3]	S_{BET}/S_{cal}	Hg (%)	Ac[4]	S_r/S_t[5]	r[6]
SB1	5.72	202	0.63	17.87	3.12	0.50	1.20
SB2	11.45	404	0.20	42.22	3.86	0.59	0.34
SB3	16.42	580	0.13	65.53	3.99	0.64	0.20
SB4	20.68	730	0.08	79.90	3.86	0.62	0.13
SB5	23.28	822	0.06	79.89	3.42	0.55	0.11
SPG1	11.43	403	0.19	41.31	3.61	0.58	0.33
SPG2	17.64	623	0.10	54.96	3.12	0.50	0.20
SPG3	23.88	843	0.06	51.85	2.17	0.35	0.17
SPG4	25.77	909	0.06	55.02	2.13	0.34	0.17
SPG5	25.86	913	0.04	73.33	2.84	0.45	0.09
SPS1	11.63	410	0.20	27.84	2.39	0.38	0.52
SPS2	13.76	486	0.15	26.16	1.90	0.30	0.50
SPS3	18.10	639	0.11	31.51	1.74	0.28	0.40
SPS4	22.41	791	0.06	27.03	1.21	0.19	0.32
SPS5	26.60	939	0.04	20.89	0.79	0.13	0.31

[1] Abbreviations as in Table 1.
[2] For sample identification, see text.
[3] S_{cal} = surface of the deposited sulfur using 150 $Å^2$ as cross-sectional area of the sulfur molecule following Klein and Henning (1984), see text.
[4] Ac: specific activity, g Hg retained per g S loaded.
[5] S_r/S_t: reactive sulfur fraction.
[6] r: ratio between values of columns 4 and 7. See text.

https://doi.org/10.1346/CCMN.1991.0390102 Published online by Cambridge University Press

Table 6. Mercury adsorption of palygorskite based adsorbents.[1]

Sample[2]	S (%)	S_{cal} (m^2/g)[3]	S_{BET}/S_{cal}	Hg (%)	Ac[4]	S_r/S_t[5]	r[6]
PN1	12.11	427	0.13	50.69	4.19	0.67	0.19
PN2	15.92	562	0.09	42.50	2.67	0.43	0.20
PN3	21.89	772	0.06	46.83	2.14	0.34	0.18
PN4	25.02	883	0.05	42.50	1.70	0.27	0.19
PT1	12.88	455	0.16	51.91	4.03	0.65	0.25
PT2	16.04	566	0.12	53.00	3.30	0.53	0.23
PT3	22.14	781	0.08	60.44	2.73	0.44	0.18
PT4	23.99	847	0.06	62.52	2.61	0.42	0.14
RBS1	10.00	353	1.22	16.90	1.69	0.27	4.52

[1] Abbreviations as in Table 1.
[2] For sample identification, see text.
[3] S_{cal} = surface of the deposited sulfur using 150 Å^2 as cross-sectional area of the sulfur molecule following Klein and Henning (1984), see text.
[4] Ac: specific activity, g Hg retained per g S loaded.
[5] S_r/S_t: reactive sulfur fraction.
[6] r: ratio between values of columns 4 and 7. See text.

rosity. Sulfur deposition on these short fibers was gradual, and macroporosity was preserved through sulfurization.

A direct relationship between surface area and reactivity cannot be abstracted from Tables 5 and 6. Column 3 (S_{cal}) lists the theoretical surface area occupied by the sulfur load, using 150 Å as the cross-sectional area of the sulfur molecule, following Klein and Henning (1984). In column 4, the ratio S_{BET}/S_{cal} decreases with increasing sulfur load. The fraction of inactive sulfur for N_2 adsorption increases with loading, suggesting an accumulation of sulfur on the substrates, which eventually clogged the pores and hindered gas diffusion towards the active surface.

Reactivity was apparently not directly related to macroporosity either, inasmuch as samples having small macropore volume showed more specific activity than others having a pore volume several times greater: cf., for example, sample SB3 (V_{MP} 0.080 cm^3/g) with sample PT2 (V_{MP} 1.024 cm^3/g), both having an activity of about 3.99. In contrast, samples SB5 and SPS4, each having a similar sulfur content, surface area, and macropore volume, showed quite different specific activity, 3.42 and 1.21, respectively.

Not even a direct relation between reactivity and mesoporosity was found; samples having similar sulfur load, surface area, and mesopore volumes (e.g., samples SB2, SPG1, and SPS1) showed quite different activities. Apparently pore distribution was more important. Thus, samples SB2 and SPG1 having quite similar pore distribution (Figure 4a) had almost the same activity in mercury retention (3.86 and 3.61, respectively), whereas sample SPS1, which had a different pore distribution, had a much lower specific activity (2.39). Also, samples SPS2 and PT2 which differed only in pore distribution (Figure 4b) had activities (1.90 and 3.32, respectively), which were possibly related to a lower content of small pores ($r < 30$ Å) in the former. Series PN also showed a significant decrease in activity for sulfur loads >15%, which may be related to a parallel decrease in the number of small pores (Daza *et al.*, 1987).

The need for pore widths >60 Å is probably related to the formation of HgS, a bulky molecule which, on forming in the pore mouths, hindered the progress of the mercury vapors entering the pores. As a result, pore size distribution, more than total porosity or surface area, is apparently more important in explaining the reactivity of the samples. Steijns (1976), working with microporous activated carbon, concluded that a degree of micropore filling of about 50% yielded the best mercury adsorbents. This is only a partial view of the problem. The fact is, that the optimum in activity depends on the remaining pore size distribution once the sulfur has been loaded, as has been found for sepiolite and palygorskite, which are still good adsorbents when the micropore volume is nearly saturated with sulfur (see Tables 3 and 4). For a given sulfur load, chemisorption will proceed as long as room still exists for mercury to diffuse and be incorporated as mercury sulfide inside the porous network of the adsorbent.

Influence of the allotropic states of deposited sulfur

Local chemical analysis taken by EDX from different samples and spots show important differences in Hg/S ratio. The atomic ratio Hg/S vs. atomic ratio S/Si for samples SB5 and SPS5, for example, is shown in Figure 5. A high S/Si value means very thick sulfur films on the silicate substrate, whereas high Hg/S values mean a high capacity of the deposited sulfur for mercury chemisorption (the maximum being 1). As can be seen, similar S/Si values for different samples do not necessarily mean similar reactivity. Confirming the results in Table 5, the steeper slope for sample SPS5 corresponds to a greater decrease in reactivity of the deposited sulfur compared with sample SB5.

https://doi.org/10.1346/CCMN.1991.0390102 Published online by Cambridge University Press

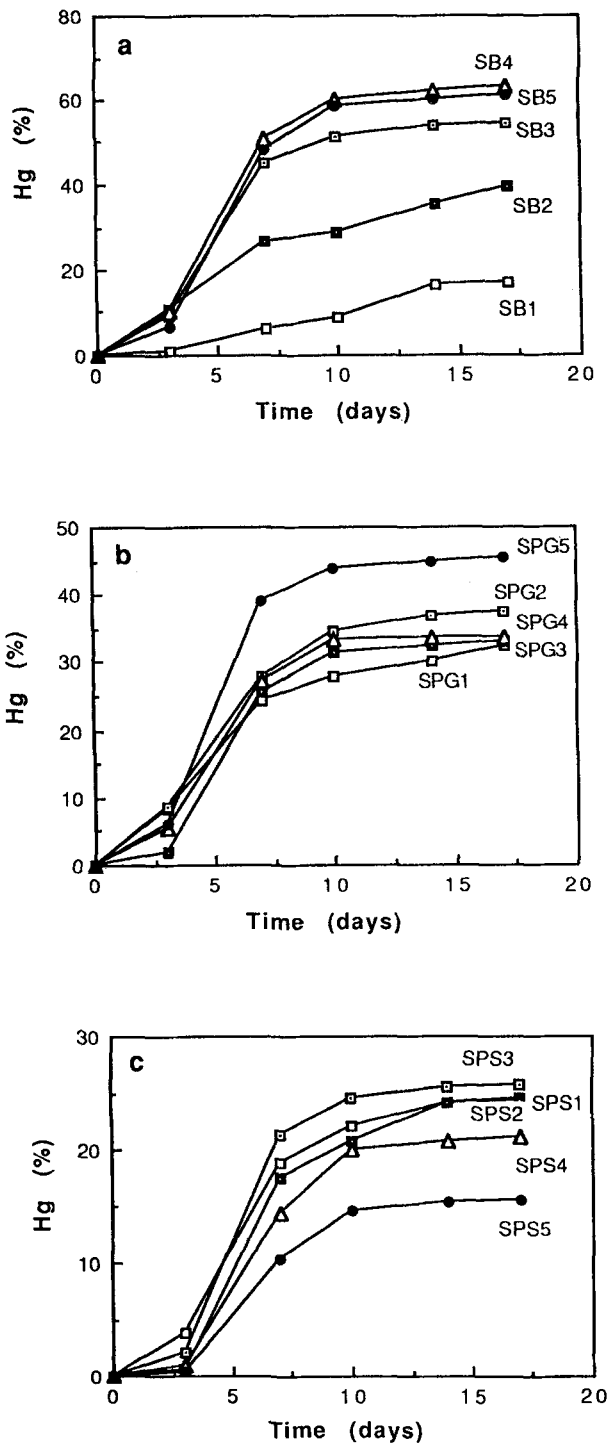


Figure 2. Mercury chemisorption on sulfurized sepiolite: a. SB series: □ SB1; ■ SB2; ⊡ SB3; △ SB4; ● SB5. b. SPG series: □ SPG1; ■ SPG2; ⊡ SPG3; △ SPG4; ● SPG5. c. SPS series: □ SPS1; ■ SPS2; ⊡ SPS3; △ SPS4; ● SPS5.

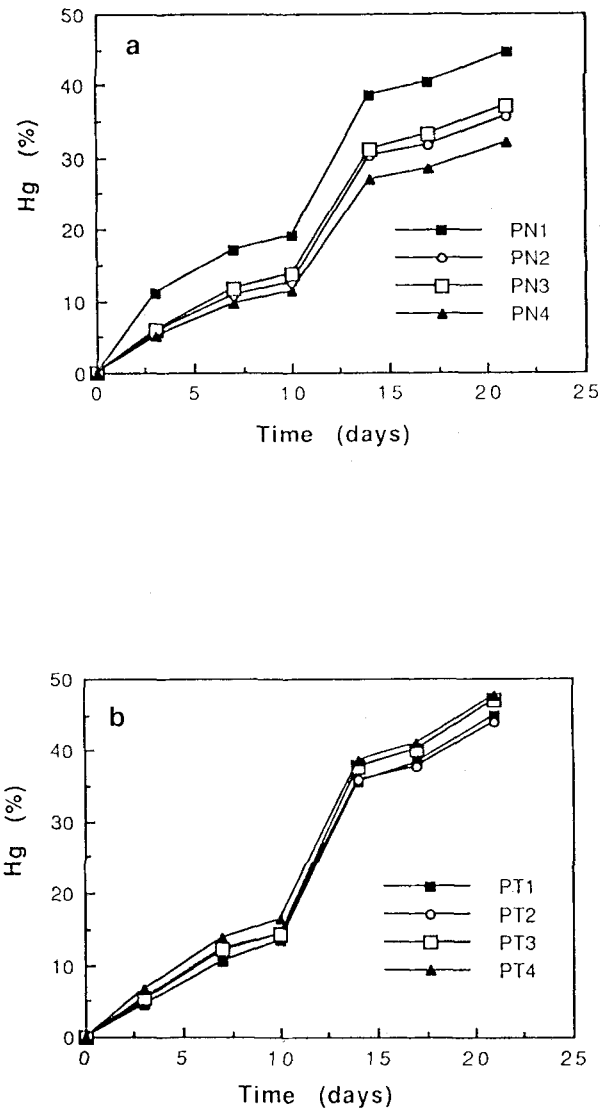
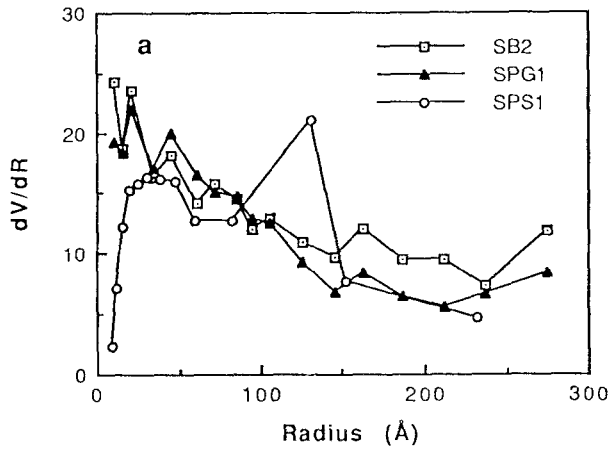


Figure 3. Mercury chemisorption on sulfurized palygorskite: a. PN series: ■ PN1; ○ PN2; □ PN3; ▲ PN4. b. PT series: ■ PT1; ○ PT2; □ PT3; ▲ PT4.

On the other hand, S_{BET}/S_{cal} in column 4 of Tables 5 and 6 does not follow the trend shown by S_r/S_t (ratio of reactive sulfur to total sulfur) in column 7. If the reactivity was related exclusively to the texture, the ratio between the values of columns 4 and 7 (r, column 8) would be constant, which clearly is not the case. As no steric hindrance exists for Hg (r ~ 1.45 Å) with respect to N_2 (r ~ 2.27 Å), a new factor must come into play to explain this behavior, especially the maximum found for samples SB3 or SPG5, or the extremely high values for samples PN1 or PT1.

As it is already known, sulfur can exist in a variety of allotropic states depending on temperature, physical state, and preparative process. If hydrogen sulfide oxidation is used as a source of sulfur formation, the

https://doi.org/10.1346/CCMN.1991.0390102 Published online by Cambridge University Press



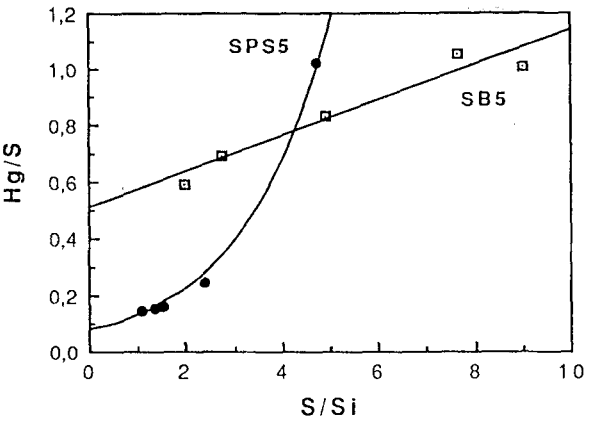


Figure 5. Atomic ratio Hg/S vs. S/si based on energy-dispersive X-ray data. ⊡ sample SB5; ● SPS5.

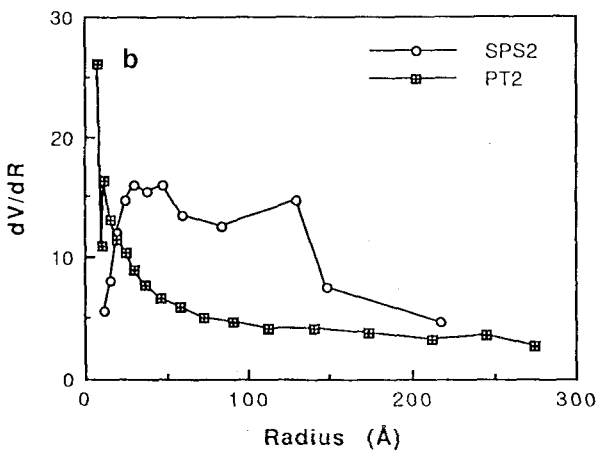


Figure 4. Pore size distributions for: a. Samples ⊡ SB2; ▲ SPG2; ○ SPS1. b. Samples ⊞ PT2; ○ SPS2.

exothermicity of the reaction (~220 kJ/mole), together with the refractory character of the support, results in a rise in temperature—the more reactive the surface of the solid, the more important the rise. The process takes place on the active sites of the surface (Daza *et al.*, 1989), spreading out on it and filling the pores from the small to larger ones. Meyer (1964) suggested that under these reaction conditions, the coexistence of three different allotropic states, Sλ (octocycles), Sπ (8-members linear chains), and Sμ (n-members linear chains), their relative proportions depending on temperature and texture of the support. At temperatures >160°C linear species prevail, with chain length depending on temperature; at temperatures <120°C, cyclic species are more abundant. On sulfur condensation (Kelvin), the pores, depending on their size, accommodate cyclic or linear S chains, which remain trapped, with no possibility of recombination or change by steric hindrance once the reaction is finished and the sample is cooled. Because the heat of dissociation for a linear S–S bond is 53.9 kcal/mole (Anonymous, 1953) vs. ~64 kcal/mole for a cyclic bond (Meyer, 1964), the resulting initial reactivity will depend on the proportion of linear or cyclic sulfur on the sample. On HgS formation through mercury chemisorption, 92 kcal/mole evolve (Tuller, 1954). This energy in turn, can break down new S–S bonds (more in linear chains than in octocyclic molecules), making the reaction progress easier as more terminal sulfur is produced. This means that, if octocyclic Sλ has mainly been deposited, an induction period may be necessary before the adsorbent reaches an optimum in activity in order to break enough S–S bonds to secure the progress of the reaction, such as can be seen in Figure 2.

SUMMARY AND CONCLUSIONS

Most of the sulfurized fibrous silicates prepared in this work by catalytic oxidation of H_2S are more active in scavenging mercury vapor than conventional sulfurized activated carbon, with a similar sulfur load. The pore size distribution and surface reactivity of the materials are quite suitable for sulfur retention, giving rise to values as high as 30%.

The activity of the resulting sulfurized adsorbents is related chiefly to the accessibility and also to the chemical reactivity of the deposited sulfur. Inasmuch as linear chains of sulfur are more frequently formed at higher temperatures and on larger pore sizes, more active sites on the solid or higher velocity in sulfur production may result in higher activity for demercuriation, provided the dispersion of the deposited sulfur is adequate. In that sense, the higher reactivity of some samples (samples PN1 and PT1 with respect to sample SB1, Figure 2) can be explained. As sulfurization progresses, be-

https://doi.org/10.1346/CCMN.1991.0390102 Published online by Cambridge University Press

cause the deposited terminal sulfur acts as a catalyst for the oxidation reaction (Steijns and Mars, 1974), no difference should be expected in the demercuriating behavior of all fibrous silicates, except that derived from sulfurization temperature and accessibility of the active sulfur present. Especially long particles, as in micronized sepiolite samples, which are quite suitable for sulfur retention, produce a deletereous effect on mercury retention by forming a "shell" of sulfur, which hinders the diffusion of reacting gases inside the adsorbent mass.

REFERENCES

ACGIH (1987–1988) Threshold limit values and biological exposure indices for 1987–1988: American Conference of Governmental Industrial Hygienist.

Anonymous (1953) Gmelins Handbuch Der Anorganischen Chemie (1953) Vol. 9, Teil A. Verlag Chemie GMBH, Weinheim, p. 569.

Brunauer, S., Skalny, J., and Odler, I. (1973) Complete pore structure analysis: in *Proc. Int. Symp. RILEM/IUPAC* Prelim. Rept.—Part I, S. Modry and M. Soata, eds., Acad. Praga. C-3, pp. 26.

Daza, L. (1986) Silicatos sulfurados para eliminación de vapores de mercurio: Ph.D. thesis, Univ. Complutense, Madrid, Spain, p. 20.

Daza, L., Mendioroz, S., Pajares, J. A., and Palacios, J. M. (1987) Sulphurized diatomite as a potential demercuriating agent: *React. Solids* **3,** 351–364.

Daza, L., Mendioroz, S., and Pajares, J. A. (1987) Sulphurized, attapulgites as mercury vapour adsorbents: in *Proc. 31st Int. Cong. of Pure and Applied Chem.*, IUPAC '87 P3 7.29, Bulgarian Acad. of Sciences, Sofia, Bulgaria.

Daza, L., Mendioroz, S., and Pajares, J. A. (1989) Influence of texture and chemical composition on sulfur deposition onto sepiolites: *Appl. Clay Sci.* **4,** 389–402.

Klein, J. and Henning, K. D. (1984) Catalytic oxidation of hydrogen sulfide on activated carbon: *Fuel* **63,** 1064–1067.

Langmyhr, F. J. and Paus, P. E. (1968) The analysis of Inorganic Siliceous materials by AAS and the HF decomposition technique. Part 1: *Anal. Chim. Acta* **43,** 397–408.

Lovett, W. D. and Cunniff, F. T. (1974) Air pollution control by activated carbon: *Chem. Eng. Progr.* **70,** 43–47.

Mendioroz, S., Daza, L., and Pajares, J. A. (1986) Procedimiento de fabricación de un adsorbente azufrado util para retener vapores de metal como mercurio: *Spanish Patent* **551862,** Feb. 11, 1986, 10 pp.

Meyer, B. (1964) Solid allotropes of sulfur: *Chem. Rev.* **64,** 429–451.

Pierce, C. (1953) Computation of pore sizes from physical adsorption data: *J. Phys. Chem.* **57,** 149–152.

Sinha, R. K. and Walker, P. L. (1972) Removal of mercury by sulfurized carbons: *Carbon* **10,** 754–756.

Steijns, M. (1976) The catalytic oxidation of hydrogen sulfide on porous materials: Ph.D. thesis, Twente University of Technology, Enschede, The Netherlands, p. 55.

Steijns, M. and Mars, P. (1974) The role of sulfur trapped in micropores in the catalytic partial oxidation of hydrogen Sulfide with Oxygen: *J. Catal.* **35,** 11–17.

Steijns, M., Peppelenbos, A., and Mars, P. (1976) Mercury chemisorption by sulfur adsorbed in porous materials: *J. Colloid Interface Sci.* **57,** 181–186.

Tuller, W. N. (1954) *The Sulfur Data Book:* McGraw-Hill Inc., New York, p. 67.

(Received 19 July 1989; accepted 8 October 1990; MS. 1927)

https://doi.org/10.1346/CCMN.1991.0390102 Published online by Cambridge University Press